



mTOR Complex 1 Regulates Lipin 1 Localization to Control the SREBP Pathway

Timothy R. Peterson,¹ Shomit S. Sengupta,¹ Thurl E. Harris,³ Anne E. Carmack,³ Seong A. Kang,¹ Eric Balderas,¹ David A. Guertin,⁴ Katherine L. Madden,⁵ Anne E. Carpenter,⁵ Brian N. Finck,⁶ and David M. Sabatini^{2,*}

¹Whitehead Institute for Biomedical Research

²Whitehead Institute for Biomedical Research, Howard Hughes Medical Institute

Koch Center for Integrative Cancer Research at MIT, Department of Biology, Massachusetts Institute of Technology, Cambridge, MA 02142, USA

³Department of Pharmacology, University of Virginia, Charlottesville, VA 22908, USA

⁴Program in Molecular Medicine, University of Massachusetts Medical School, Worcester, MA 01605, USA

⁵Imaging Platform, Broad Institute of Harvard and MIT, Cambridge, MA 02142, USA

⁶Division of Geriatrics and Nutritional Sciences, Washington University School of Medicine, St. Louis, MO 63110, USA

*Correspondence: sabatini@wi.mit.edu

DOI 10.1016/j.cell.2011.06.034

SUMMARY

The nutrient- and growth factor-responsive kinase mTOR complex 1 (mTORC1) regulates many processes that control growth, including protein synthesis, autophagy, and lipogenesis. Through unknown mechanisms, mTORC1 promotes the function of SREBP, a master regulator of lipo- and sterogenic gene transcription. Here, we demonstrate that mTORC1 regulates SREBP by controlling the nuclear entry of lipin 1, a phosphatidic acid phosphatase. Dephosphorylated, nuclear, catalytically active lipin 1 promotes nuclear remodeling and mediates the effects of mTORC1 on SREBP target gene, SREBP promoter activity, and nuclear SREBP protein abundance. Inhibition of mTORC1 in the liver significantly impairs SREBP function and makes mice resistant, in a lipin 1-dependent fashion, to the hepatic steatosis and hypercholesterolemia induced by a high-fat and -cholesterol diet. These findings establish lipin 1 as a key component of the mTORC1-SREBP pathway.

INTRODUCTION

The mechanistic target of rapamycin (mTOR) is an evolutionarily conserved serine/threonine kinase that has an essential role in cell growth (Wullschleger et al., 2006). Genetic and biochemical studies into the mechanism of action of rapamycin, which has emerged as a valuable immunosuppressive and anticancer drug (Abraham and Eng, 2008), led to the discovery of TOR as its intracellular target (Brown et al., 1994; Chiu et al., 1994; Heitman et al., 1991; Sabatini et al., 1994).

Rapamycin was initially noted for its antifungal activity as it potently inhibited diverse amino acid, nucleic acid, and lipid-utilizing metabolic processes (Singh et al., 1979). Since the iden-

tification of TOR, it has become increasingly appreciated that its kinase activity is critical to several growth processes, including protein synthesis. The effects of mTORC1 in translation are thought to be controlled through rapamycin-sensitive phosphorylation of its substrates, S6 kinase 1 (S6K1) and eIF4E-binding protein 1 (4E-BP1) (Brown et al., 1995; Brunn et al., 1997; Hara et al., 2002; Kim et al., 2002). Recently, the role of mTORC1 in regulating translation was recast by the finding that rapamycin, which allosterically partially inhibits mTOR kinase activity (Brown et al., 1995), does not inhibit 4E-BP1 phosphorylation equally well in all cell contexts despite invariably promoting S6K1 dephosphorylation (Choo et al., 2008; Feldman et al., 2009; Thoreen et al., 2009). On the other hand, catalytic site ATP-competitive mTOR inhibitors, such as Torin1, suppress both S6K1 and 4E-BP1 phosphorylation regardless of cell context (Liu et al., 2010; Thoreen et al., 2009). In addition to translation, catalytic site mTOR inhibitors, also potently regulate other known outputs of mTORC1 signaling, such as autophagy and proliferation, to a greater degree than rapamycin does (Dowling et al., 2010; Feldman et al., 2009; Thoreen et al., 2009). These results suggest that in viewing rapamycin as a complete mTORC1 inhibitor, other mTORC1-dependent phenotypes might have eluded detection.

The mTOR pathway regulates several anabolic and catabolic pathways at the mRNA expression level (Düvel et al., 2010; Porstmann et al., 2008). Critical to the regulation of fatty acid and cholesterol biosynthetic gene expression is the SREBP family of transcription factors (Horton et al., 2002). The SREBP family is comprised of three isoforms: SREBP-1a, SREBP-1c, and SREBP-2 (hereafter collectively referred to as SREBP unless stated otherwise; SREBP-1a and SREBP-1c are encoded by the same gene, SREBP-1, and differ in their first exon; SREBP-2 is a distinct gene) (Horton et al., 2002). Studies by Brown, Goldstein, and colleagues have elucidated key parts of the mechanism by which cholesterol sensing is coupled to the activity of SREBP (Brown and Goldstein, 2009). Previous work shows that mTORC1 positively regulates the activity of SREBP-1 (Düvel

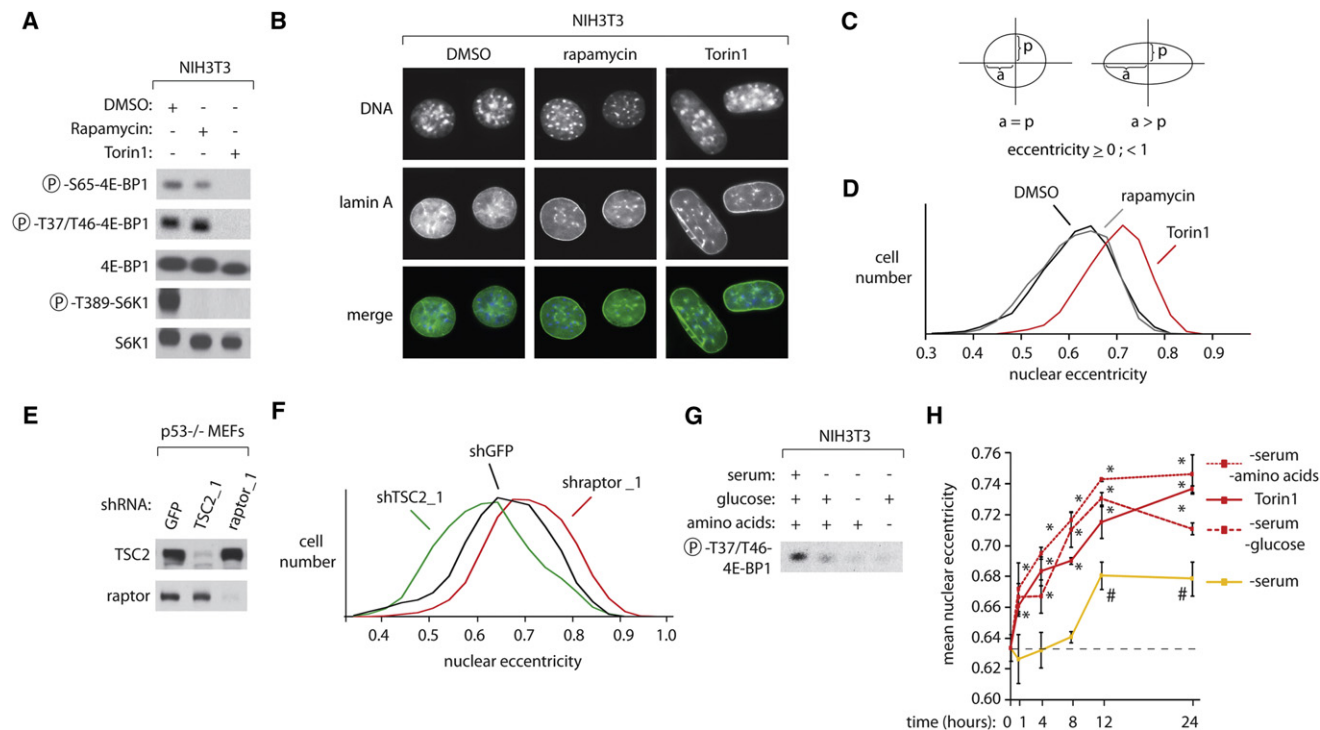


Figure 1. mTORC1 Regulates Nuclear Eccentricity in a Rapamycin-Resistant Manner

(A) NIH 3T3 cells treated with 100 nM rapamycin, 250 nM Torin1, or vehicle for 12 hr were analyzed by immunoblotting for the phosphorylation states and levels of the indicated proteins.

(B) NIH 3T3 cells treated with 100 nM rapamycin, 250 nM Torin1, or vehicle for 12 hr were processed in an immunofluorescence assay to detect lamin A (green), costained with DAPI for DNA content (blue), and imaged. Illustrative nuclei for each condition are shown.

(C) Explanation of eccentricity. The eccentricity of an elliptical object is a measure of how much the shape of the ellipse deviates from being circular. Defined mathematically, $\text{eccentricity} = 1 - 2/((a/p) + 1)$, where a is the radius at apopsis, i.e., the farthest distance from the edge of the ellipse to its center, and p is the radius at periapsis, i.e., the closest distance to ellipse center. The eccentricity of an ellipse is necessarily between 0 and 1; a circle has an eccentricity of 0. As the eccentricity tends to 1, the ellipse becomes more elongated, and the ratio of a/p tends to infinity.

(D) Images processed in (B) were analyzed for nuclear eccentricity based on lamin A immunofluorescence by image analysis software (Carpenter et al., 2006). Nuclear eccentricity distributions of rapamycin- and Torin1-treated cells were overlaid with those from corresponding vehicle-treated cells. Mean eccentricity values for three independent fields for each condition (>500 cells total) are as follows: DMSO (black) 0.630; rapamycin (gray) 0.628; Torin1 (red) 0.704.

(E) Immunoblot analysis of TSC2 and raptor protein levels in $p53^{-/-}$ mouse embryonic fibroblasts (MEFs) with RNAi-mediated knockdown of a control protein, TSC2, or raptor.

(F) $p53^{-/-}$ MEFs with knockdown of TSC2, raptor, or a control protein were analyzed as in (D). Mean eccentricity values for three independent fields for each condition (>500 cells total) are as follows: shGFP (black) 0.660; shTSC2_1 (green) 0.622; shraprator_1 (red) 0.705.

(G) Immunoblot analysis of T37/T46 4E-BP1 phosphorylation in NIH 3T3 cells deprived of serum, serum and glucose, or serum and amino acids for 12 hr.

(H) NIH 3T3 cells treated with 250 nM Torin1 or deprived of serum, serum and glucose, or serum and amino acids for the indicated times were analyzed as in (D). The mean eccentricity value for untreated cells is 0.633 (dashed line). Error bars indicate standard error for $n = 3$. * indicates $p < 0.03$; # indicates $p < 0.01$.

See also Figure S1.

et al., 2010; Li et al., 2010; Porstmann et al., 2008). However, the finding that rapamycin does not affect SREBP target gene expression in all cellular contexts (Moule et al., 1995; Sharpe and Brown, 2008) suggests that the mechanisms through which mTORC1 regulates SREBP are complex and not yet fully understood.

RESULTS

mTORC1, Nutrients, and Growth Factors Regulate Nuclear Eccentricity

With the impetus that Torin1 causes greater mTORC1 inactivation than rapamycin, we looked for mTORC1-dependent pheno-

types that might be largely resistant to rapamycin but sensitive to Torin1. By visually inspecting NIH 3T3 cells treated with Torin1, which as expected potently inhibits the phosphorylation at the mTORC1-catalyzed sites on 4E-BP1 and S6K1 and T37/T46 and T389, respectively (Figure 1A), we observed that their nuclei, including the nuclear matrix component lamin A, as well as DNA, dramatically changed in their circumferential shapes (Figure 1B). Rapamycin, although abolishing T389 S6K1 phosphorylation (Figure 1A), lacked an effect on nuclear shape, and this correlated with its inability to inhibit T37/T46 4E-BP1 phosphorylation (Figures 1A and 1B). In geometric terms, it appeared that Torin1 increased nuclear eccentricity, a property that when referring to circular objects is defined by the lengths of the major and minor

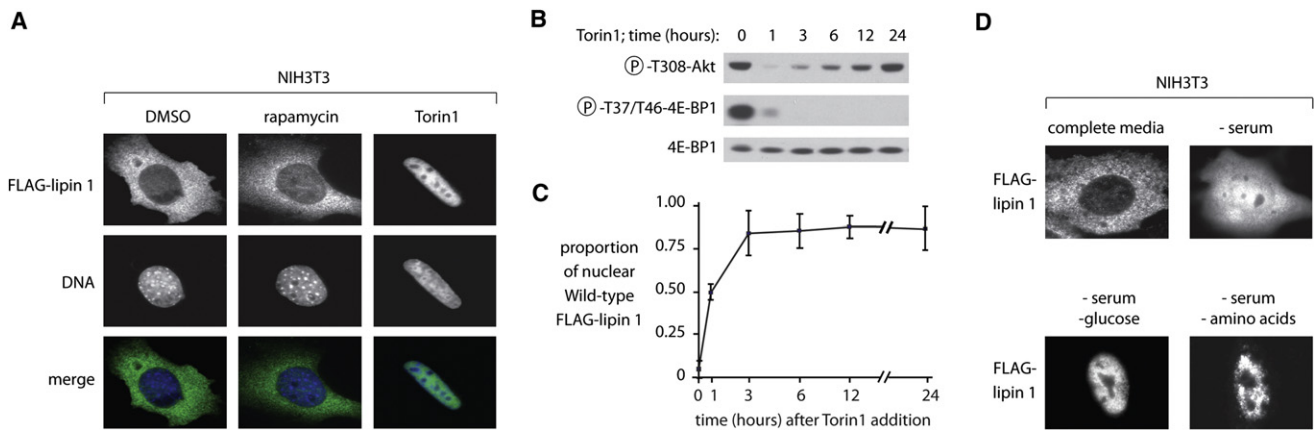


Figure 2. Lipin 1 Cytoplasmic-Nuclear Distribution Is Regulated by mTORC1, Growth Factors, and Nutrients

(A) NIH 3T3 cells overexpressing FLAG-lipin 1 were treated with 100 nM rapamycin, 250 nM Torin1, or vehicle for 8 hr. Cells were then processed in an immunofluorescence assay to detect FLAG (green), costained with DAPI for DNA content (blue), and imaged.

(B) FLAG-lipin 1-overexpressing NIH 3T3 cells were treated with 250 nM Torin1 for the specified times and analyzed by immunoblotting for the phosphorylation states and levels of the indicated proteins.

(C) Cells treated as in (B) were processed in an immunofluorescence assay to detect FLAG, costained with DAPI for DNA content, and imaged. The overlap of FLAG immunoreactivity with DAPI staining was analyzed for >500 cells total. Error bars indicate standard error for $n = 3$.

(D) NIH 3T3 cells overexpressing FLAG-lipin 1 were grown in complete media or deprived of serum, serum and glucose, or serum and amino acids for 8 hr and imaged as in (A).

See also Figure S2.

axes, the apoptosis (a) and periapsis (p), respectively (Figure 1C and Figure S1A available online). Quantification of nuclei treated with either of the mTOR inhibitors confirmed what was visibly apparent (Figure 1B), that is, that Torin1 causes a substantial increase in nuclear eccentricity compared with rapamycin or vehicle treatment (Figure 1D). The effects of Torin1 are likely to be mTORC1 dependent as knockdown of the essential mTORC1 component, raptor, which positively regulates mTORC1 signaling (Hara et al., 2002; Kim et al., 2002), increased nuclear eccentricity, whereas depletion of the mTORC1 pathway negative regulator, TSC2, (Goncharova et al., 2002), decreased nuclear eccentricity (Figures 1E and 1F). The effect of Torin1 on nuclear eccentricity was also mimicked by the dual PI3K/mTOR inhibitor LY294002 but not by other agents that promote a G1 arrest, such as a double thymidine block or inhibition of MAPK signaling (Figures S1B and S1C), suggesting that nuclear eccentricity is regulated in an mTORC1-dependent manner independently of cell-cycle progression.

Correlating with inhibition of 4E-BP1 phosphorylation (Figure 1G), combined serum and glucose deprivation increased nuclear eccentricity similar to Torin1 or raptor knockdown (Figures 1D and 1F) in a time-dependent manner (Figure 1H). However, serum starvation alone, which partially inhibited 4E-BP1 phosphorylation (Figure 1G), modestly increased nuclear eccentricity (Figure 1H). These results suggest that nuclear eccentricity is a cellular property that is dynamically regulated by mTORC1 activity and environmental conditions.

mTORC1, Growth Factors, and Nutrients Regulate Lipin 1 Localization

In investigating whether others have previously observed regulation of nuclear eccentricity, we noted that the overexpression of

the Ned1 gene product in *Schizosaccharomyces pombe* promotes this phenotype (Tange et al., 2002). This finding was interesting to us because, previously, the mammalian Ned1 homolog, lipin 1, was shown to be phosphorylated in a nutrient- and growth factor-stimulated, rapamycin-sensitive manner (Huffman et al., 2002). However, at the time it was not known whether lipin 1 regulated nuclear eccentricity, or what the function of the mTOR-dependent lipin 1 phosphorylation might be.

Because rapamycin lacks an effect on lipin 1 phosphatidic acid phosphatase (PAP1) activity (Harris et al., 2007), we considered that mTOR might control some other aspect of lipin 1 function such as its localization. Strikingly, treatment of NIH 3T3 or AML12 hepatocyte cells with Torin1 caused a complete redistribution of recombinant lipin 1 from the cytoplasm to the nucleus (Figure 2A and Figure S2A). Rapamycin, on the other hand, largely lacked an effect on recombinant lipin 1 localization (Figure 2A and Figure S2A), and this correlated with a lack of effect on 4E-BP1 phosphorylation (Figure 1A). That rapamycin lacked an effect on lipin 1 localization is in disagreement with that recently observed in 3T3-L1 adipocytes (Péterfy et al., 2010). However, as the completeness of inhibition of rapamycin on mTORC1 signaling varies considerably between cell types (Choo et al., 2008), we reasoned that this discrepancy on lipin 1 localization might be explained by the differing rapamycin sensitivities of mTORC1 in the cell types assessed. In support of this, in HEK293T cells, unlike in NIH 3T3 cells (Figure 1A and Figure 2A), lipin 1 nuclear translocation and S65 4E-BP1 phosphorylation were partially sensitive to rapamycin (Figures S2B and S2C). As with recombinant lipin 1, Torin1 or combined serum and amino acid or glucose deprivation, but not rapamycin, caused strong nuclear relocalization of endogenous lipin 1 (Figure S2D).

It was possible that the effects of Torin1 on lipin 1 nuclear translocation might require inhibition of mTORC2/PI3K concomitantly with or independently of inhibiting mTORC1 (Jacinto et al., 2004; Peterson et al., 2009; Sarbassov et al., 2004; Thoreen et al., 2009). To address this, we monitored the time dependence of Torin1 treatment on lipin 1 localization. After acute treatment (1 hr), correlating with the downregulation of mTORC1 as well as mTORC2/PI3K signaling, as judged by T308 Akt phosphorylation at this early time point, lipin 1 partially accumulated in the nucleus (Figures 2B and 2C). However, at later times (≥ 3 hr), despite mTORC2/PI3K activity being restored, lipin 1 was fully retained in the nucleus, and this correlated with the maintained impairment of mTORC1 signaling (Figures 2B and 2C). Torin1 also caused lipin 1 nuclear translocation to the same extent in rictor-deficient cells as in those containing intact mTORC2 (Figure S2E), which together with the above results suggests that lipin 1 cytoplasmic-nuclear relocalization responds to mTORC1 and not mTORC2 status.

Unlike serum deprivation alone, serum deprivation combined with glucose or amino acid deprivation promoted the full nuclear accumulation of lipin 1 (Figure 2D and Figure S2D). Similarly, in HEK293T cells, amino acid deprivation caused complete lipin 1 nuclear accumulation (Figure S2F). LY294002 or the AMPK-activating compound AICAR, which strongly impair mTORC1 signaling, also promoted complete lipin 1 nuclear translocation (Figure S2G). Lastly, because the phosphorylation states of lipin 1, lipin 2, and Pah1/Smp2 are regulated by cell-cycle activity (Grimsey et al., 2008; O'Hara et al., 2006), we tested whether various cell-cycle perturbations affect lipin 1 localization. However, neither G1 arrest by a double thymidine block, CDK inhibition, nor MAPK inhibition affected lipin 1 localization (Figure S2G). Taken together, these results suggest that lipin 1 cytoplasmic retention is positively promoted by mTORC1.

mTORC1 Directly Phosphorylates Lipin 1 to Regulate Lipin 1 Localization and Nuclear Eccentricity

We sought to gain insight into the mechanisms through which mTORC1 regulates lipin 1 translocation. Because mTORC1 is a protein kinase, we focused on the lipin 1 phosphorylation state and the 19 phosphorylation sites previously identified on it (Harris et al., 2007). In our mass spectrometry analysis, we detected 17 of the 19 published sites as well as 2 novel sites, S237 and T335. Nine of the sites fall within "proline-directed" motifs (S/T-P) (Figure 3A) like those in 4E-BP1 that are directly phosphorylated by mTOR (Brunn et al., 1997; Burnett et al., 1998; Gingras et al., 1999). We raised antibodies to 2 of the proline-directed sites, S106 and S472, and confirmed their phosphospecificities using a form of lipin 1 in which we mutated the serine and threonine residues to alanines at 17 of the 19 sites, including S106 and S472 (hereafter referred to as "17xS/T \rightarrow A lipin 1") (Figure S3A). Rapamycin mostly inhibited and Torin1 completely inhibited S106 lipin 1 phosphorylation, which is a pattern similar to the effect of these inhibitors on S65 4E-BP1 phosphorylation (Figure 3B, Figure S3B). On the contrary, S472 lipin 1 phosphorylation, like T37/T46 4E-BP1 phosphorylation, was largely insensitive to rapamycin but sensitive to Torin 1 (Figure 3B, Figure S3B). Interestingly, a prolonged

course (12 hr) of Torin1, but not rapamycin, impaired S237 and S472 lipin 1 phosphorylation (Figure S3C). Also comparable to 4E-BP1 phosphorylation, combined serum and nutrient deprivation strongly downregulated lipin 1 S106 and S472 phosphorylation, whereas serum deprivation alone only partially inhibited lipin 1 phosphorylation at these same sites (Figure 3C). Therefore, similar to the effect of mTORC1 on the 4E-BP1 phosphorylation state, nuclear eccentricity, and lipin 1 localization, mTORC1 activity regulates lipin 1 multisite phosphorylation in a graded manner.

Whereas T389 S6K1 can be efficiently phosphorylated in vitro by mTOR in the absence of raptor, T37/T46 4E-BP1 phosphorylation requires raptor (Hara et al., 2002; Yip et al., 2010). Because lipin 1 phosphorylation was similar to 4E-BP1 phosphorylation in terms of its rapamycin and Torin1 sensitivities (Figure 3B), we sought to determine whether lipin 1 can be directly phosphorylated at S106 and S472 in an mTORC1-dependent manner and whether mTOR might also require raptor to phosphorylate lipin 1. To test this, we isolated mTOR via the mTORC1 component, mLST8/G β L (Kim et al., 2003), from control or raptor knockdown cells and performed in vitro kinase assays on purified lipin 1. An mTORC1-containing mLST8/G β L purification, but not one where raptor was depleted in cells by RNAi and/or inhibited with Torin1, readily phosphorylated S106 and S472 lipin 1 and T37/T46 4E-BP1 (Figure 3D and Figure S3D). We observed similar results on S106 lipin 1 using mTORC1 highly purified via gel filtration (Yip et al., 2010) (Figure S3E). Importantly, wild-type lipin 1 was highly phosphorylated by mTORC1 (compare with the mTORC1 substrate S6K1), whereas mutation of its 17 sites virtually abolished the ability of mTORC1 to phosphorylate it (Figure S3F). Lastly, as multiple TORC1 substrates remain bound to TORC1 when purified from cells (Lempiäinen et al., 2009; Schalm et al., 2003), we assessed lipin 1 for this behavior. Indeed, raptor and coexpressed raptor and mTOR copurified with lipin 1 but not with the metap2 or rap2a control proteins (Figure S3G). That lipin 1 did not interact with mTOR alone and that mTOR did not increase the abundance of raptor copurifying with lipin 1 suggest that lipin 1 interacts with mTORC1 via raptor. Taken together, the above data suggest that mTORC1 is a bona fide lipin 1 kinase.

Because mTORC1 kinase activity regulates lipin 1 localization, we reasoned that a mechanism through which lipin 1 localization might be regulated is by its phosphorylation at mTORC1-catalyzed sites. Mutation of only the rapamycin-sensitive-catalyzed site, S106, to alanine did not affect the lipin 1 cytoplasmic-nuclear distribution (Figure 3E). Whereas, mutating 6 of the 19 lipin 1 sites (2 of the 7 proline-directed sites) caused partial lipin 1 redistribution (Figure 3E). Lastly, mutation of all 17 lipin 1 sites to alanine, including S106 and S472, was sufficient to promote the full lipin 1 nuclear accumulation (Figure 3E and Figure S3H). Therefore, inactivation of mTORC1 leads to nuclear lipin 1 sequestration by a mechanism that requires its dephosphorylation at numerous mTORC1-regulated sites.

As the 17xS/T \rightarrow A mutant lipin 1 recapitulated the effects of mTORC1 inactivation on lipin 1 localization, we determined whether lipin 1 might regulate the effects of mTORC1 on nuclear eccentricity. Indeed, the time-dependent increases in nuclear eccentricity caused by Torin1 in cells containing lipin 1

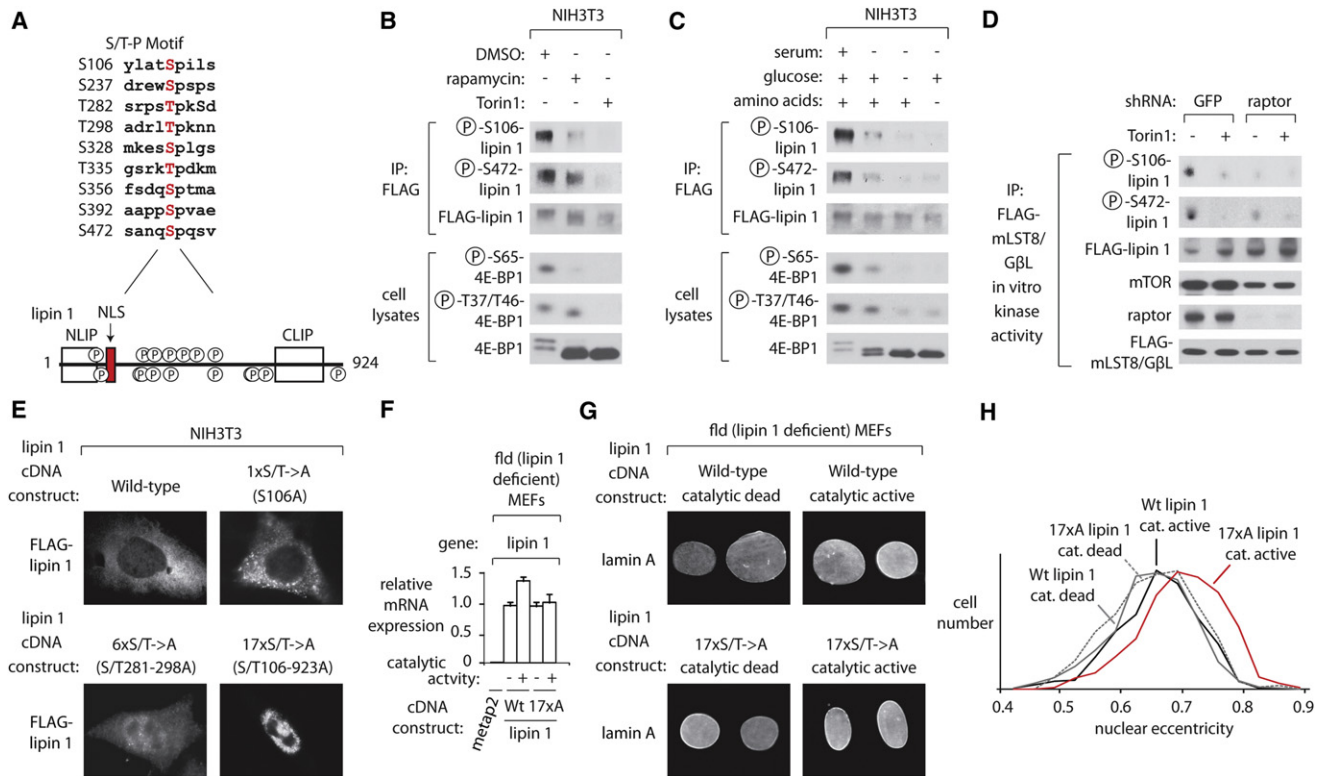


Figure 3. mTORC1-Catalyzed Lipin 1 Phosphorylation Regulates Lipin 1 Localization and Nuclear Eccentricity

(A) Schematic of the location of lipin 1 phosphorylation sites. NLIP, N-terminal lipin 1 conserved region. CLIP, C-terminal lipin 1 conserved region. NLS, nuclear localization signal (in red). Capitalized serine or threonine residues (in red) indicate the lipin 1 phosphorylation sites that are followed in the +1 position by a proline residue.

(B) NIH 3T3 cells transfected with FLAG-lipin 1 were treated with 100 nM rapamycin, 250 nM Torin1, or vehicle for 4 hr. FLAG immunoprecipitates and cell lysates were analyzed by immunoblotting for the phosphorylation states and levels of the specified proteins.

(C) NIH 3T3 cells transfected with FLAG-lipin 1 were grown in complete media or deprived of serum, serum and glucose, or serum and amino acids for 4 hr.

(D) HEK293T cells overexpressing FLAG-mLST8/GβL were infected with lentivirus expressing an shRNA targeting raptor or GFP. FLAG immunoprecipitates were analyzed for mTOR kinase activity toward lipin 1 in the presence of 250 nM Torin1 or vehicle.

(E) FLAG-wild-type, 1xS/T → A, 6xS/T → A, and 17xS/T → A lipin 1-overexpressing NIH 3T3 cells were processed in an immunofluorescence assay to detect FLAG and imaged.

(F) Indicated FLAG-tagged lentiviral expression vectors were stably introduced into fld cells and RNA was isolated 5 days post-infection. All mRNAs were measured by qRT-PCR and normalized to 36B4 mRNA levels. Error bars indicate standard error for n = 4.

(G) Each lipin 1-expressing cell line generated as in (F) was processed in an immunofluorescence assay to detect lamin A and imaged.

(H) Images processed in (G) were analyzed for nuclear eccentricity as in Figure 1D. Mean eccentricity values for three independent fields for each condition (>500 cells total) are as follows: catalytic dead, wild-type lipin 1 (gray) 0.666; catalytic dead, 17xS/T → A lipin 1 (gray hatched line) 0.671; catalytically active, wild-type lipin 1 (black) 6.76; catalytically active, 17xS/T → A lipin 1 (red) 0.713.

See also Figure S3.

were absent in lipin 1-deficient (fld, fatty liver dystrophy) cells (Péterfy et al., 2001) (Figure S3I). We next stably expressed either the catalytically active or inactive forms of the wild-type (cytoplasmic) or the 17xS/T → A mutant (nuclear) lipin 1 in fld cells. While mutation of the 17 phosphorylation sites on lipin 1 did not affect PAP1 activity (Figure S3J), nor did lipin 1 catalytic activity affect its localization (Figure S3K), the expression of the catalytically active, nuclear-localized 17xS/T → A mutant lipin 1, but not its catalytic dead or the wild-type form, was sufficient to increase nuclear eccentricity (Figures 3F– 3H). These results suggest that the effects of mTORC1 on nuclear eccentricity are driven, at least in part, by the catalytic activity of nuclear-localized lipin 1.

Repression of SREBP-Dependent Transcription by Constitutively Dephosphorylated and Nuclear-Localized Lipin 1

Because lipin 1 regulates lipid homeostasis (Finck et al., 2006; Han et al., 2006; Rehnmark et al., 1998), we were interested in whether nuclear-localized lipin 1 might contribute to the regulation by mTORC1 of lipid biosynthetic gene expression. The SREBP pathway was an attractive transcriptional pathway to investigate because the cell-type-specific effects of rapamycin on lipin 1 localization (Figure 2B and Figure S2B) were reminiscent of those on SREBP target gene expression (Düvel et al., 2010; Moule et al., 1995; Porstmann et al., 2008; Sharpe and Brown, 2008).

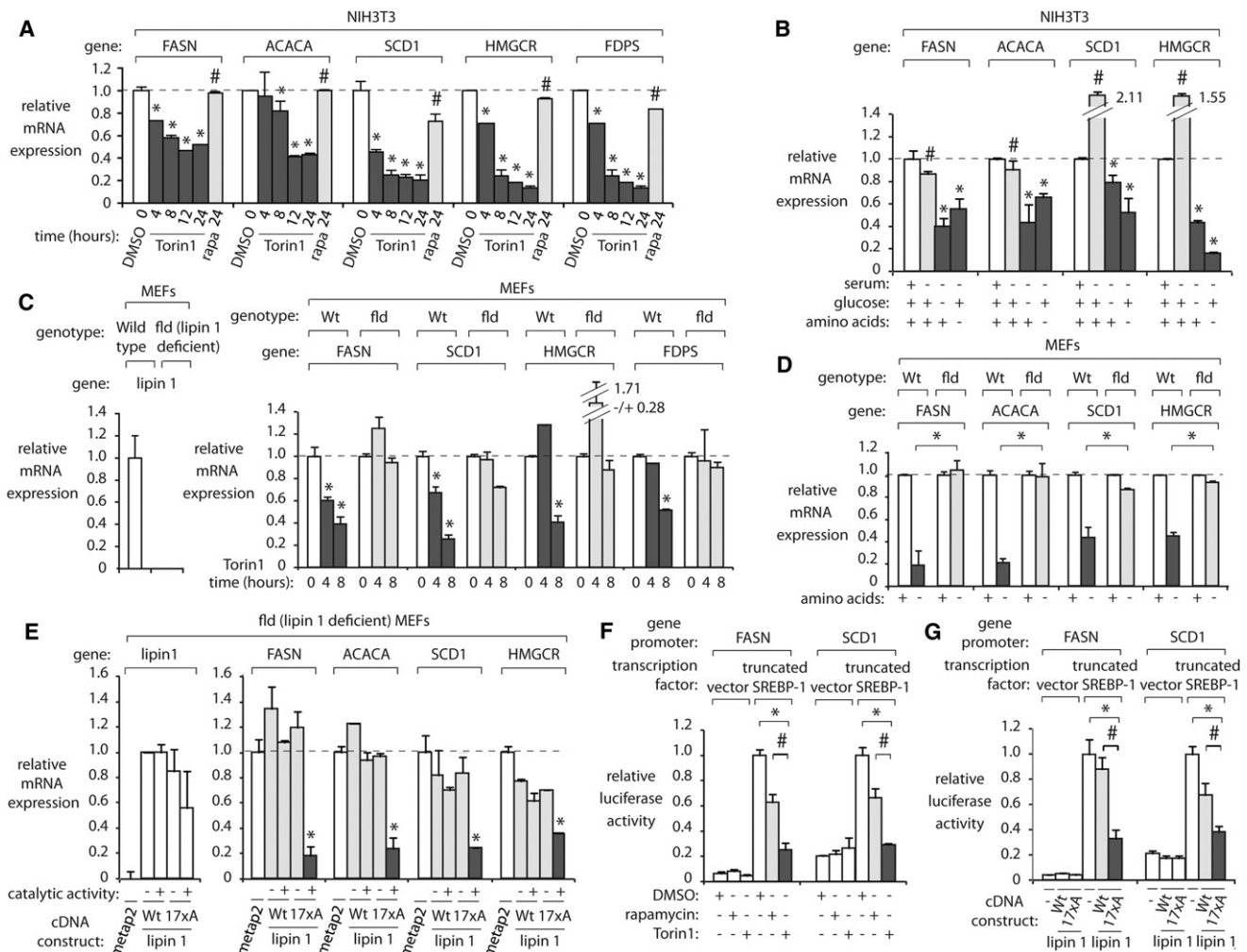


Figure 4. mTORC1-Regulated Lipin 1 Relocalization Is Necessary and Sufficient to Repress SREBP-Dependent Transcription

(A) NIH 3T3 cells were treated with 100 nM rapamycin, 250 nM Torin1, or vehicle for the indicated times. All mRNAs were measured by qRT-PCR and normalized to 36B4 mRNA levels. Error bars indicate standard error for $n = 4$. * indicates $p < 0.04$; # indicates $p < 0.02$.

(B) NIH 3T3 cells were grown in complete media, deprived of serum, serum and glucose, or serum and amino acids for 12 hr. All mRNAs were analyzed as in (A). Error bars indicate standard error for $n = 4$. * indicates $p < 0.02$; # indicates $p < 0.03$.

(C) Wild-type or fld MEFs were treated with 250 nM Torin1 or vehicle for the indicated times. All mRNAs were measured by qRT-PCR and normalized to 36B4 mRNA levels. * indicates $p < 0.02$.

(D) Wild-type or fld MEFs were deprived of serum or serum and amino acids for 8 hr. All mRNAs were analyzed as in (C). * indicates $p < 0.01$.

(E) Indicated FLAG-tagged lentiviral expression vectors were stably introduced into fld cells and RNA was isolated 5 days post-infection. All mRNAs were analyzed as in (A). * indicates $p < 0.007$.

(F) HepG2 cells were cotransfected with expression constructs containing a transcriptionally active, truncated form of SREBP-1 along with a construct containing a SREBP-1-responsive promoter of either the FASN or SCD1 genes tethered to luciferase cDNA and treated with 20 nM rapamycin, 250 nM Torin1, or vehicle for 4 hr. Luciferase measurements for each promoter activity reporter were normalized to those of SREBP-1-transfected, vehicle-treated cells. * indicates $p < 0.001$; # indicates $p < 0.01$.

(G) HepG2 cells cotransfected as in (F) were additionally transfected with empty vector, wild-type lipin 1, or 17xS/T \rightarrow A lipin 1. * indicates $p < 0.0001$; # indicates $p < 0.02$.

See also Figure S4.

We first determined to what extent rapamycin and Torin1 regulated the mRNA expression of numerous genes that are known to be induced by SREBP-1 and/or SREBP-2, such as fatty acid synthase (FASN), acetyl-CoA carboxylase alpha (ACACA), stearoyl CoA-desaturase (SCD1), HMG-CoA reductase (HMGCR), and farnesyl diphosphate synthase (FDPS) (Horton et al., 2003).

In a time-dependent manner, Torin1 strongly downregulated all SREBP targets we examined, yet rapamycin was largely ineffective at decreasing the expression of these same targets at the latest time point (Figure 4A). Neither Torin1 nor rapamycin decreased SREBP-1 mRNA, whereas both inhibitors downregulated SREBP-2 mRNA to a comparable extent (Figure S4A).

Similar to the effects of Torin1, serum and glucose or amino acid deprivation strongly downregulated SREBP target gene expression compared with cells grown in complete media or deprived only of serum (Figure 4B). Correlating with the differential strengths of these mTORC1-regulating inputs on lipin 1 localization, these results suggest that the redistribution of cytoplasmic lipin 1 to the nucleus might be important in the regulation of SREBP target gene expression by mTORC1. To test this, we monitored SREBP target mRNA levels in the presence or absence of Torin1 in wild-type and fld cells. At time points after which Torin1 caused lipin 1 to fully enter the nucleus (Figure 2C), fld cells were completely refractory to the effects of Torin1 on SREBP target expression (Figure 4C) without differentially regulating SREBP-1 mRNA levels (Figure S4B). Complementary to these findings, lipin 1 deficiency prevented the reduction in SREBP target gene expression caused by amino acid deprivation (Figure 4D).

We measured SREBP target gene expression in fld cells in which we stably expressed either the wild-type or the constitutively dephosphorylated, nuclear-localized 17xS/T→A mutant lipin 1. Whereas wild-type lipin 1 had little or no effect on SREBP target mRNA levels, the 17xS/T→A lipin 1 mutant repressed, in a manner dependent on its catalytic activity, all SREBP targets examined (Figure 4E). Because it is possible that mTORC1 and lipin 1 might control SREBP target mRNA levels independently of SREBP itself, we measured the effects of mTORC1 and lipin 1 on FASN and SCD1 promoter activities driven by a truncated, nuclear-localized, transcriptionally active form of SREBP-1 (Shimano et al., 1996). Fitting with the effects of Torin1 and rapamycin on endogenous FASN and SCD1 mRNA expression (Figure 4A), Torin1 strongly impaired SREBP-1-induced, FASN and SCD1 promoter activities, yet rapamycin more modestly impaired the activities of these same reporters (Figure 4F and Figure S4C). Similarly, 17xS/T→A lipin 1, unlike wild-type lipin 1, potently downregulated both FASN and SCD1 promoter activities (Figure 4G). These results establish lipin 1 as both necessary and sufficient for mediating the effects of mTORC1 inhibition on SREBP transcriptional activity.

mTORC1-Dependent Regulation of Nuclear SREBP Protein Abundance Is Mediated by Lipin 1

Because mTORC1 promotes the expression of the mature, nuclear (Düvel et al., 2010; Porstmann et al., 2008), as well as a truncated, constitutively active form of the SREBP-1 protein (Figure S4C), we asked whether lipin 1 might regulate the effects of mTORC1 on nuclear SREBP protein levels. In nuclear extracts from Torin1-treated cells, SREBP protein levels were largely ablated after only 4 hr of treatment and were maintained at very low levels up to 12 hr (Figure 5A). On the contrary, rapamycin only weakly reduced nuclear SREBP protein levels at all time points tested, and neither inhibitor downregulated cytoplasmic SREBP-1 levels (Figure 5A). Knockdown of SREBP-1 in multiple cell types strongly downregulated both SREBP target gene expression as well as SREBP-2 mRNA expression (Düvel et al., 2010) (Figures S5A and S5B) suggesting that the reduction in cytoplasmic SREBP-2 protein levels caused by mTORC1 inhibition (Figure 5A) could be due to mTORC1-dependent regulation of SREBP-1 on SREBP-2 mRNA levels. Nuclear SREBP protein

levels were also strongly downregulated by combined serum and glucose or amino acid deprivation in comparison to cells given complete media or deprived only of serum (Figure 5B). Confirming the generality of these findings, in HEK293T cells, Torin1 or amino acid starvation strongly reduced nuclear SREBP protein expression (Figures S5C and S5D). To test a role for lipin 1 in mediating the effects of mTORC1 on nuclear SREBP protein, we assessed nuclear SREBP levels in wild-type and lipin 1-deficient cells after Torin1 treatment. In contrast to lipin 1-containing cells, fld cells were highly resistant to the effects of Torin1 on nuclear SREBP protein levels (Figure 5C). To assess whether mTORC1-controlled localization of lipin 1 is critical to these effects, we measured nuclear SREBP protein levels in cells expressing the wild-type or the 17xS/T→A mutant lipin 1. The 17xS/T→A mutant, but not wild-type lipin 1 or the control protein, metap2, repressed nuclear SREBP protein expression in multiple cell types (Figure 5D, Figures S5E and S5F). Taken together, these results establish the constitutively dephosphorylated, nuclear form of lipin 1 as both necessary and sufficient for mediating the effects of mTORC1 inhibition on the expression of nuclear SREBP proteins.

A growing body of work suggests that A-type lamins colocalize with transcriptional regulators (Johnson et al., 2004; Wilson and Foissner, 2010). However, less is known about how the localizations of these transcription factors are regulated. Because mTORC1-dependent changes in lipin 1 localization strongly altered the structure of the lamin A-containing nuclear matrix and because lamin A is known to bind SREBP (Lloyd et al., 2002), we considered whether the localization of SREBP might be important in the mTORC1- and lipin 1-dependent regulation of its nuclear depletion. In untreated cells, full-length SREBP-1 and SREBP-2 appeared diffusely localized throughout the cell, in agreement with a previous report (Figure 5E and Figure S5F) (Wang et al., 1994). Strikingly, in the presence of Torin1, SREBP-1 and SREBP-2 decreased in overall immunostaining intensity, consistent with our fractionation studies (Figure 5A and Figure S5C), but became concomitantly enriched at the nuclear periphery (Figure 5E and Figure S5G) and partially colocalized with lamin A (Figure 5E). Expression of the constitutively nuclear 17xS/T→A lipin 1 (Figure S5H), in contrast to wild-type lipin 1, also caused marked turnover of nuclear SREBP-1 that was associated with residual SREBP-1 partially colocalizing with lamin A (Figure 5F and Figure S5H). Interestingly, these mTORC1- and lipin 1-regulated changes in SREBP immunostaining are similar to those seen in cells expressing lipodystrophy-causing lamin A mutations or treated with lipodystrophy-inducing medications that alter lamin A distribution (Capanni et al., 2005; Caron et al., 2003). Thus, mTORC1- and lipin 1-dependent changes in SREBP nuclear abundance correlate with its redistribution into proximity to lamin A at the nuclear periphery.

Lipin 1 Is Required for the Effects of mTORC1 on the SREBP Pathway and Lipid Homeostasis in Mice

To test a role for mTORC1 and lipin 1 in the regulation of the SREBP pathway in a physiologically meaningful context, we deleted raptor in the postnatal liver in floxed raptor mice by expressing Cre recombinase under the control of the Albumin

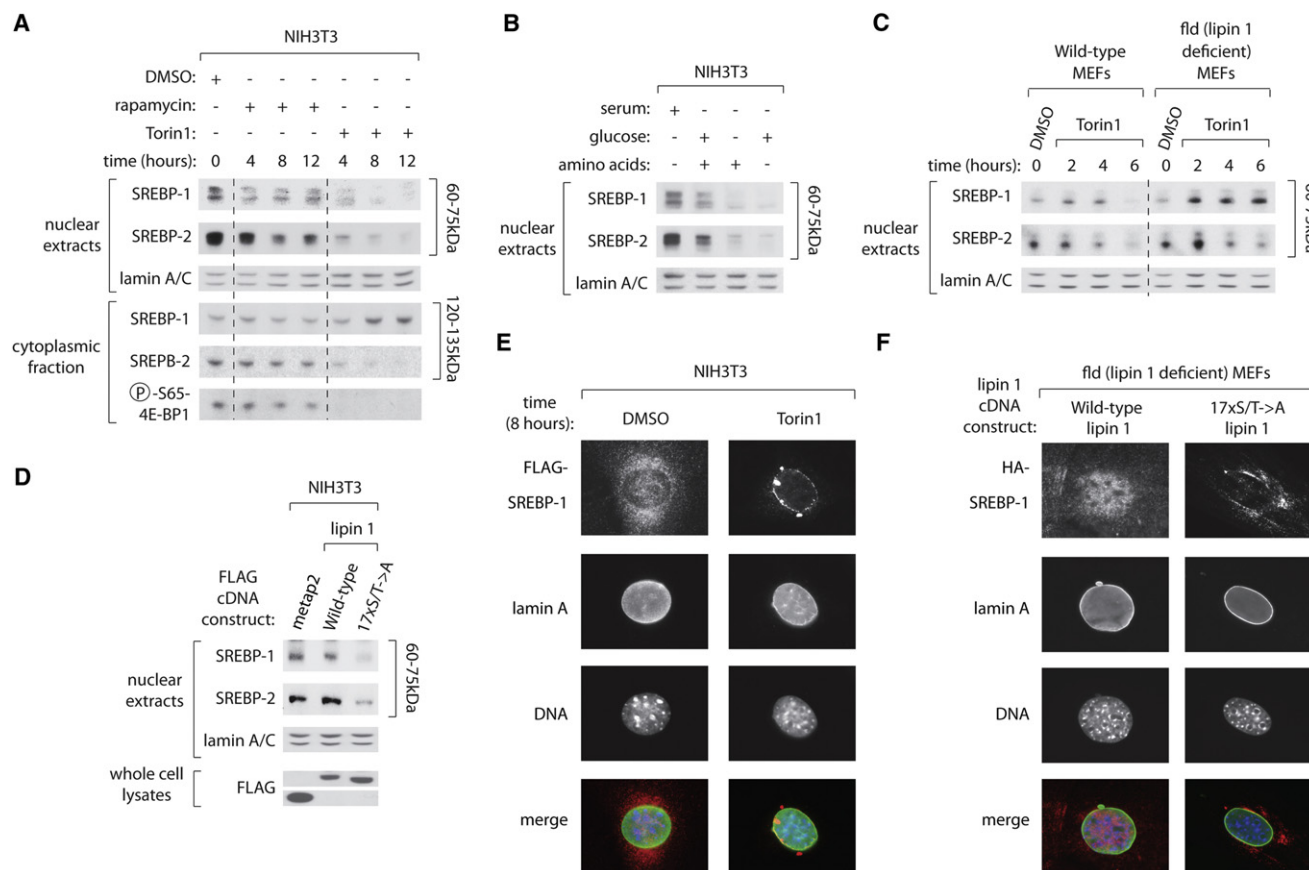


Figure 5. Constitutively Dephosphorylated, Nuclear Lipin 1 Decreases Nuclear SREBP Protein Abundance

(A) NIH 3T3 cells were treated with 20 nM rapamycin, 250 nM Torin1, or vehicle for the indicated times, cytoplasmic and nuclear fractions were isolated, and the levels of the indicated proteins were analyzed by immunoblotting.

(B) NIH 3T3 cells were grown in complete media or deprived of serum, serum and glucose, or serum and amino acids for 4 hr and analyzed as in (A).

(C) Wild-type or fld MEFs were treated with 250 nM Torin1 or vehicle for the indicated times and analyzed as in (A).

(D) Indicated FLAG-tagged lentiviral expression vectors were stably introduced into NIH 3T3 cells and analyzed as in (A).

(E) NIH 3T3 cells overexpressing FLAG-SREBP-1 were treated with 250 nM Torin1 or vehicle for 8 hr. Cells were then processed in an immunofluorescence assay to detect FLAG (red) and lamin A (green), costained with DAPI for DNA content (blue), and imaged.

(F) fld cells coexpressing HA-SREBP-1 and wild-type or 17xS/T→A mutant lipin 1 were processed in an immunofluorescence assay to detect HA (red) and lamin A (green), costained with DAPI for DNA content (blue), and imaged.

See also Figure S5.

promoter (Sengupta et al., 2010). We first confirmed that S106 and S472 lipin 1 phosphorylation are regulated by mTORC1-regulating inputs in hepatocytes and that raptor expression, mTORC1, and PI3K/Akt signaling were altered specifically in the livers of albumin-CRE⁺; floxed raptor mice (Li-Rap^{KO}) (Figures S6A and S6B, Figure 6A). Surprisingly, despite strongly perturbing mTORC1/PI3K signaling in their livers, Li-Rap^{KO} mice developed normally and at 4 months of age were of comparable body weight as wild-type, control (Ctrl) mice (Figure S6C). Therefore, we challenged the wild-type and Li-Rap^{KO} mice with a high-fat and high-cholesterol “Western” diet. The effects of raptor loss were now clear: unlike with chow-feeding, where both groups gained weight at a similar rate, Western diet-fed Li-Rap^{KO} mice gained substantially less weight than wild-type animals despite similar food intake (Figures S6C and S6D). The fasted livers of Western diet but not chow-fed Li-Rap^{KO} mice

were also substantially reduced in size and were less yellowish in appearance and disorganized by intracellular droplets compared with the fasted livers of control mice (Figure 6B). We next measured SREBP target gene expression in chow- and Western diet-fed wild-type and Li-Rap^{KO} mice. As expected, the expression of FASN and HMGCR were repressed by raptor loss, though the degree of inhibition was substantially greater on the Western diet, particularly for FASN (Figure 6C). The elevations in liver triglycerides and plasma cholesterol in wild-type animals on the Western compared with the chow diet were also largely blocked by raptor loss (Figure 6D), results that, notably, phenocopy those seen in SREBP-1c knockout mice (Kalaany et al., 2005).

We suspected that lipin 1 would be important in the resistance of Li-Rap^{KO} animals to some of the phenotypic consequences caused by the Western diet because fld fibroblasts were

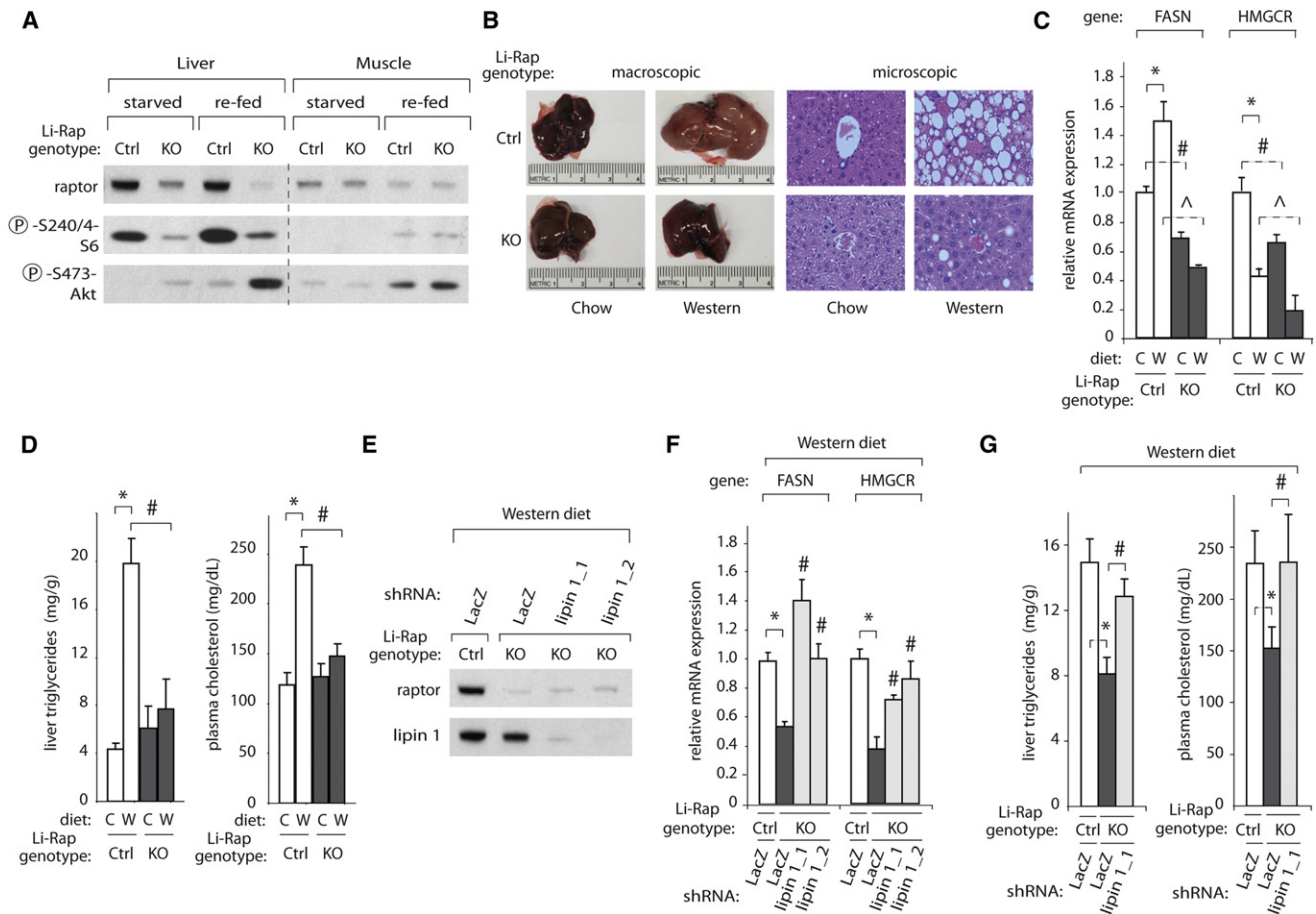


Figure 6. Response of Liver-Specific Raptor Knockout Mice to a High-Fat and High-Cholesterol (Western) Diet Is Lipin 1 Dependent
 (A) Control (floxed raptor; Albumin-CRE^{-/-}, abbreviated Ctrl) and Li-Rap^{KO} (floxed raptor; Albumin-CRE^{+/+}) were starved of chow overnight and re-fed for 45 min. Liver and muscle tissue lysates were prepared and analyzed by immunoblotting for the phosphorylation states and levels of specified proteins.
 (B) Representative 1× or 20× images of control and Li-Rap^{KO} livers taken from chow and Western diet-fed mice.
 (C) Liver tissue was isolated and RNA was extracted from the indicated mice fed their respective diets for 6–8 weeks. All mice were starved for 4 hr prior to liver harvesting. All mRNAs were measured by qRT-PCR and normalized to 36B4 mRNA levels. Error bars indicate standard error for n = 4–6. C, chow; W, Western. * indicates p < 0.02, #p < 0.04, ^p < 0.05.
 (D) Liver tissue from which lipids were extracted and plasma for cholesterol measurements were obtained from mice fed the indicated diets for 6–8 weeks and starved 4 hr prior to sample harvesting. Error bars indicate standard error for n = 4 (liver triglycerides), n = 6 (plasma cholesterol). * indicates p < 0.004, # indicates p < 0.05.
 (E) Western diet-fed control and Li-Rap^{KO} were infected with adenovirus-expressing shRNAs targeting lacZ or lipin 1. Liver was harvested 5 days after infection and lysates prepared, and immunoblotting was performed for the indicated proteins.
 (F) mRNA was isolated and analyzed as in (C). * indicates p < 0.01, # indicates p < 0.05 in comparing LacZ shRNA versus lipin 1 shRNA-treated Li-Rap^{KO} mice.
 (G) Liver triglycerides and plasma cholesterol were measured as in (D). * indicates p < 0.05, # indicates p < 0.05.
 See also Figure S6.

resistant to the effects of Torin1 on SREBP target gene expression (Figure 4C). Indeed, using two distinct adenovirally delivered shRNAs to lipin 1, we depleted lipin 1 from the livers of Western diet-fed Li-Rap^{KO} mice (Figure 6E), and this largely restored SREBP target gene expression to the levels seen in control mice (Figure 6F). Correspondingly, the levels of liver triglycerides and plasma cholesterol in Western diet-fed Li-Rap^{KO} mice were also re-elevated after the lipin 1 knockdown to those in control mice (Figure 6G). Therefore, the SREBP pathway in the liver is positively regulated by mTORC1 in a manner that is opposed by lipin 1, and this regulation is critical for the development of

hepatic steatosis and hypercholesterolemia caused by prolonged high-fat and high-cholesterol feeding.

DISCUSSION

Our findings provide insight into how mTORC1 regulates SREBP transcriptional activity and are consistent with a model in which loss of mTORC1-mediated lipin 1 phosphorylation promotes its nuclear entry and promotes the downregulation of nuclear SREBP protein (Figure 7). This model suggests several interesting avenues for future exploration. Regarding the role of

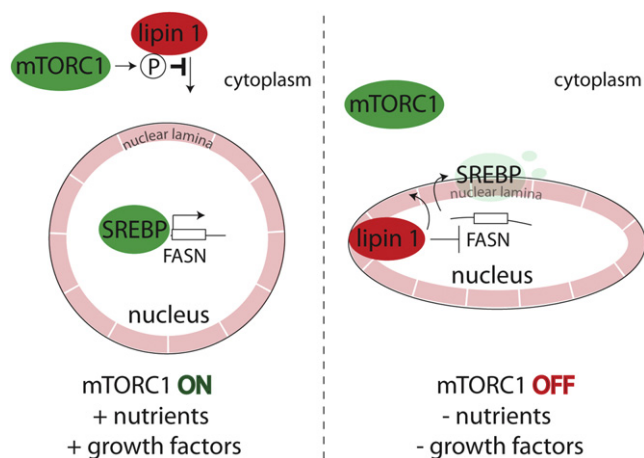


Figure 7. Model of mTORC1/Lipin 1-Dependent Regulation of SREBP Transcriptional Activity

mTORC1 in regulating lipin 1 phosphorylation-dependent changes in its localization, it will be interesting to determine the relative rapamycin sensitivities of each lipin 1 phosphorylation site. As S472 lipin 1 phosphorylation appears to be partially rapamycin sensitive (Figure 3B), it is possible that this and the other sites we have characterized do not represent the key rapamycin-resistant site(s) modified by mTORC1 during multi-site lipin 1 phosphorylation. However, that multiple lipin 1 sites are at least partially rapamycin resistant (Figure 3B, Figures S3B and S3C) and that mutation of six lipin 1 phosphorylation sites causes partial lipin 1 nuclear translocation (Figure 3E) suggest an alternative conclusion to a strict hierarchical phosphorylation model. That is, perhaps the differential effects of rapamycin versus Torin1 on lipin 1 function reflect the additive effect of more extensive dephosphorylation of lipin 1 by Torin1 at each of the multiple sites targeted by mTORC1. It also remains unknown how mTORC1/lipin 1 regulates SREBP nuclear protein levels. Interestingly, with mTORC1 inactivation or expression of nuclear-localized lipin 1, we often observed residual SREBP in proximity to lamin A as aggregates (Figures 6D and 6E, Figure S6G) whose morphology and localization resembled lysosomes (Yu et al., 2010). As mTORC1 is known to regulate nuclear SREBP levels independently of the proteasome (Düvel et al., 2010), it will be interesting in the future to explore whether a lysosome-requiring autophagic process is involved in the mTORC1- and lipin 1-regulated turnover of nuclear SREBP.

It was interesting that mTORC1- and lipin 1-dependent changes in nuclear eccentricity correlated with their effects on SREBP transcriptional activity because one of the structural components of the nuclear matrix, lamin A, has several established connections with the SREBP pathway: (1) lamin A physically interacts with SREBP-1 and SREBP-2, and its overexpression downregulates the mRNA expression of the adipogenic SREBP target, PPAR γ 2 (Boguslavsky et al., 2006; Lloyd et al., 2002); (2) lamin A mutations in humans commonly result in a lipodystrophy, a condition characterized by abnormal adipose tissue that is also seen in adipocyte-specific SREBP-1-overex-

pressing mice (Capell and Collins, 2006; Shimomura et al., 1999). As we failed to detect a physical interaction between lipin 1 and SREBP-1 (data not shown), in the future it will be exciting to test whether lipin 1 might regulate nuclear SREBP protein via a more indirect mechanism, such as through its effects on the nuclear lamina.

Because mTORC1 promotes lipogenesis and inhibits glucose uptake (Düvel et al., 2010; Jiang et al., 2008; Porstmann et al., 2008), it is curious that rapamycin is known to cause numerous features of the metabolic syndrome: hyperlipidemia, hypercholesterolemia, and insulin resistance in humans and in mice (Blum, 2002; Cunningham et al., 2007). Considering the discrepancies we find between the effects of rapamycin and Torin1 in regulating lipin 1 and SREBP, it is clear that further examination of the differential strengths of various mTORC1 inhibitors on cellular and organismal lipid and glucose homeostasis is required. Through such work, it should be possible to determine whether potent mTORC1-inhibiting drugs could be useful as potential treatments for metabolic syndrome.

EXPERIMENTAL PROCEDURES

Materials

Reagents were obtained from the following sources: antibodies to mTOR, lamin A or lamin A/C (sc-20680, sc-6215), and SREBP-1 (sc-13551) from Santa Cruz Biotechnology; rabbit polyclonal and monoclonal antibodies to phospho-S106 lipin 1, phospho-S472 lipin 1, phospho-T389 S6K1 (cat.# 9234), phospho-T37/T46 4E-BP1 (cat.# 2855, T36/T45 for *M. musculus*), phospho-S65 4E-BP1 (cat.# 9451), and T308 Akt (cat.# 2965) from Cell Signaling Technology; rabbit polyclonal antibody to SREBP-2 from Abcam (ab30682); antibodies to lipin 1 were previously described (Huffman et al., 2002). GST-4E-BP1 was previously described (Burnett et al., 1998). Torin1 was previously described (Liu et al., 2010; Thoreen et al., 2009) and was kindly provided by Nathaniel Gray (Harvard Medical School).

Nuclear Eccentricity and Lipin 1 Nuclear-Cytoplasmic Proportion Measurements

Nuclear eccentricity was measured with CellProfiler (<http://www.cellprofiler.org>) using 10 \times images with the eccentricity measurement being made on nuclei identified by lamin A immunostaining. FLAG-lipin 1 nuclear proportion was also quantified by CellProfiler as follows: after illumination correction, the nuclei were automatically identified using the DAPI staining; the cytoplasmic compartment was defined by expanding the edges of the nuclei 20 pixels in every direction; nuclear proportion was then measured as nuclear intensity/(nuclear+cytoplasmic intensity). Further mTORC1/SREBP/lipin 1/lamin A analysis can be found at <http://www.onarbor.com>.

Immunofluorescence Assays

25,000–100,000 cells were plated on fibronectin-coated glass coverslips, fixed with 4% paraformaldehyde, and permeabilized with 0.2% Triton X-100. Permeabilized cells were blocked in 0.25% BSA PBS, incubated with primary antibody (FLAG, HA, and/or lamin A sc-20680) in blocking buffer overnight at 4°C (for detection of lipin 1 and/or lamin A) or 2 hr at room temperature (for detection of SREBP-1 or SREBP-2 and lamin A or lipin 1), and subsequently incubated with secondary antibodies (diluted in blocking buffer 1:1000) for 1 hr at room temperature. 2–4 \times PBS washes were used in between all preceding steps. The coverslips were mounted on glass slides using Vectashield containing DAPI (Vector Laboratories) and imaged with a 10 \times or 63 \times objective by using epifluorescence microscopy.

Gene Expression Analysis

Total RNA was isolated and reverse-transcription was performed from cells grown in the indicated conditions. The resulting cDNA was diluted in

DNase-free water (1:20) followed by quantification by real-time PCR. mRNA transcript levels were measured using Applied Biosystems 7900HT Sequence Detection System v2.3 software. All data are expressed as the ratio between the expression of target gene to the housekeeping genes 36B4 and/or GAPDH. Each treated sample was normalized to the level of the vehicle controls of the same cell type.

Cytoplasmic-Nuclear Fractionation

For nuclear SREBP fractionation studies, protease pellets were added to NEPER buffers (Thermo Fischer Scientific) and nuclear extracts were prepared according to the manufacturer's protocol. Whole-cell lysates were prepared by mixing matched cytoplasmic fractions and nuclear fractions.

Determination of Liver Triglycerides

Liver sections (25–50 mg) were homogenized in 900 μ l of a 2/1 chloroform/methanol mixture. The homogenate was combined with 300 μ l of methanol, vortexed, and centrifuged for 15 min at 3,000 rpm. 412.5 μ l of supernatant was transferred to a new glass tube, 200 μ l of chloroform and 137.5 μ l of 0.73% NaCl was added, and the resulting mixture was vortexed for 30 s and centrifuged at 5,000 rpm for 3 min. The upper phase was discarded and 400 μ l of a 3/48/47 mixture of chloroform/methanol/NaCl (0.58%) was added to wash the lower phase and was centrifuged at 5,000 rpm for 3 min. After three washes, the lower phase was evaporated and resuspended in 1 ml of isopropanol. Triglyceride levels were determined with a standard assay kit (Infinity Triglycerides Reagent TR22421) from Thermo Scientific according to the manufacturer's instructions. Liver triglycerides were normalized by liver section weight.

Determination of Plasma Cholesterol Content

Mouse plasma was obtained from tail vein blood, chelated with EDTA, and centrifuged at 5,000 rpm for 10 min to remove red blood cells. Levels of plasma cholesterol were determined using a standard assay kit (Infinity Cholesterol Reagent TR13421) from Thermo Scientific according to manufacturer's instructions.

SUPPLEMENTAL INFORMATION

Supplemental Information includes Extended Experimental Procedures and six figures and can be found with this article online at [doi:10.1016/j.cell.2011.06.034](https://doi.org/10.1016/j.cell.2011.06.034).

ACKNOWLEDGMENTS

We thank the following for technical assistance: We thank members of the Sabatini lab (in particular, Mathieu Laplante and Peggy Hsu), Ayce Yesilatay, and Monty Krieger for helpful discussions. D.M.S. is an investigator of the Howard Hughes Medical Institute. This work was additionally supported by grants from the National Institutes of Health (R01 AI47389 and R01 CA103866) to D.M.S.; awards from the Keck Foundation and LAM Foundation to D.M.S.; an NIH R01 GM089652-01 to A.E.C.; fellowships from the American Diabetes Association, Ludwig Cancer Fund, and Jane Coffin Childs Memorial Fund to T.R.P.; and an R01 DK078187 to B.N.F.

Received: November 11, 2010

Revised: May 17, 2011

Accepted: June 15, 2011

Published: August 4, 2011

REFERENCES

Abraham, R.T., and Eng, C.H. (2008). Mammalian target of rapamycin as a therapeutic target in oncology. *Expert Opin. Ther. Targets* *12*, 209–222.

Blum, C.B. (2002). Effects of sirolimus on lipids in renal allograft recipients: an analysis using the Framingham risk model. *Am. J. Transplant.* *2*, 551–559.

Boguslavsky, R.L., Stewart, C.L., and Worman, H.J. (2006). Nuclear lamin A inhibits adipocyte differentiation: implications for Dunnigan-type familial partial lipodystrophy. *Hum. Mol. Genet.* *15*, 653–663.

Brown, E.J., Albers, M.W., Shin, T.B., Ichikawa, K., Keith, C.T., Lane, W.S., and Schreiber, S.L. (1994). A mammalian protein targeted by G1-arresting rapamycin-receptor complex. *Nature* *369*, 756–758.

Brown, E.J., Beal, P.A., Keith, C.T., Chen, J., Shin, T.B., and Schreiber, S.L. (1995). Control of p70 s6 kinase by kinase activity of FRAP in vivo. *Nature* *377*, 441–446.

Brown, M.S., and Goldstein, J.L. (2009). Cholesterol feedback: from Schoenheimer's bottle to Scap's MELADL. *J. Lipid Res. Suppl.* *50*, S15–S27.

Brunn, G.J., Hudson, C.C., Sekulic, A., Williams, J.M., Hosoi, H., Houghton, P.J., Lawrence, J.C., Jr., and Abraham, R.T. (1997). Phosphorylation of the translational repressor PHAS-I by the mammalian target of rapamycin. *Science* *277*, 99–101.

Burnett, P.E., Barrow, R.K., Cohen, N.A., Snyder, S.H., and Sabatini, D.M. (1998). RAFT1 phosphorylation of the translational regulators p70 S6 kinase and 4E-BP1. *Proc. Natl. Acad. Sci. USA* *95*, 1432–1437.

Capanni, C., Mattioli, E., Columbaro, M., Lucarelli, E., Parnaik, V.K., Novelli, G., Wehnert, M., Cenni, V., Maraldi, N.M., Squarzonni, S., and Lattanzi, G. (2005). Altered pre-lamin A processing is a common mechanism leading to lipodystrophy. *Hum. Mol. Genet.* *14*, 1489–1502.

Capell, B.C., and Collins, F.S. (2006). Human laminopathies: nuclei gone genetically awry. *Nat. Rev. Genet.* *7*, 940–952.

Caron, M., Auclair, M., Sterlingot, H., Kornprobst, M., and Capeau, J. (2003). Some HIV protease inhibitors alter lamin A/C maturation and stability, SREBP-1 nuclear localization and adipocyte differentiation. *AIDS* *17*, 2437–2444.

Carpenter, A.E., Jones, T.R., Lamprecht, M.R., Clarke, C., Kang, I.H., Friman, O., Guertin, D.A., Chang, J.H., Lindquist, R.A., Moffat, J., et al. (2006). CellProfiler: image analysis software for identifying and quantifying cell phenotypes. *Genome Biol.* *7*, R100.

Chiu, M.I., Katz, H., and Berlin, V. (1994). RAPT1, a mammalian homolog of yeast Tor, interacts with the FKBP12/rapamycin complex. *Proc. Natl. Acad. Sci. USA* *91*, 12574–12578.

Choo, A.Y., Yoon, S.O., Kim, S.G., Roux, P.P., and Blenis, J. (2008). Rapamycin differentially inhibits S6Ks and 4E-BP1 to mediate cell-type-specific repression of mRNA translation. *Proc. Natl. Acad. Sci. USA* *105*, 17414–17419.

Cunningham, J.T., Rodgers, J.T., Arlow, D.H., Vazquez, F., Mootha, V.K., and Puigserver, P. (2007). mTOR controls mitochondrial oxidative function through a YY1-PGC-1 α transcriptional complex. *Nature* *450*, 736–740.

Dowling, R.J., Topisirovic, I., Alain, T., Bidinosti, M., Fonseca, B.D., Petroulakis, E., Wang, X., Larsson, O., Selvaraj, A., Liu, Y., et al. (2010). mTORC1-mediated cell proliferation, but not cell growth, controlled by the 4E-BPs. *Science* *328*, 1172–1176.

Düvel, K., Yecies, J.L., Menon, S., Raman, P., Lipovsky, A.I., Souza, A.L., Triantafellow, E., Ma, Q., Gorski, R., Cleaver, S., et al. (2010). Activation of a metabolic gene regulatory network downstream of mTOR complex 1. *Mol. Cell* *39*, 171–183.

Feldman, M.E., Apse, B., Uotila, A., Loewith, R., Knight, Z.A., Ruggero, D., and Shokat, K.M. (2009). Active-site inhibitors of mTOR target rapamycin-resistant outputs of mTORC1 and mTORC2. *PLoS Biol.* *7*, e38.

Finck, B.N., Gropler, M.C., Chen, Z., Leone, T.C., Croce, M.A., Harris, T.E., Lawrence, J.C., Jr., and Kelly, D.P. (2006). Lipin 1 is an inducible amplifier of the hepatic PGC-1 α /PPAR α regulatory pathway. *Cell Metab.* *4*, 199–210.

Gingras, A.C., Gygi, S.P., Raught, B., Polakiewicz, R.D., Abraham, R.T., Hoekstra, M.F., Aebersold, R., and Sonenberg, N. (1999). Regulation of 4E-BP1 phosphorylation: a novel two-step mechanism. *Genes Dev.* *13*, 1422–1437.

Goncharova, E.A., Goncharov, D.A., Eszterhas, A., Hunter, D.S., Glassberg, M.K., Yeung, R.S., Walker, C.L., Noonan, D., Kwiatkowski, D.J., Chou, M.M., et al. (2002). Tuberin regulates p70 S6 kinase activation and ribosomal protein S6 phosphorylation. A role for the TSC2 tumor suppressor gene in

- pulmonary lymphangioleiomyomatosis (LAM). *J. Biol. Chem.* **277**, 30958–30967.
- Grimsey, N., Han, G.S., O'Hara, L., Rochford, J.J., Carman, G.M., and Siniosoglou, S. (2008). Temporal and spatial regulation of the phosphatidate phosphatases lipin 1 and 2. *J. Biol. Chem.* **283**, 29166–29174.
- Han, G.S., Wu, W.I., and Carman, G.M. (2006). The *Saccharomyces cerevisiae* Lipin homolog is a Mg²⁺-dependent phosphatidate phosphatase enzyme. *J. Biol. Chem.* **281**, 9210–9218.
- Hara, K., Maruki, Y., Long, X., Yoshino, K., Oshiro, N., Hidayat, S., Tokunaga, C., Avruch, J., and Yonezawa, K. (2002). Raptor, a binding partner of target of rapamycin (TOR), mediates TOR action. *Cell* **110**, 177–189.
- Harris, T.E., Huffman, T.A., Chi, A., Shabanowitz, J., Hunt, D.F., Kumar, A., and Lawrence, J.C., Jr. (2007). Insulin controls subcellular localization and multisite phosphorylation of the phosphatidic acid phosphatase, lipin 1. *J. Biol. Chem.* **282**, 277–286.
- Heitman, J., Movva, N.R., and Hall, M.N. (1991). Targets for cell cycle arrest by the immunosuppressant rapamycin in yeast. *Science* **253**, 905–909.
- Horton, J.D., Goldstein, J.L., and Brown, M.S. (2002). SREBPs: activators of the complete program of cholesterol and fatty acid synthesis in the liver. *J. Clin. Invest.* **109**, 1125–1131.
- Horton, J.D., Shah, N.A., Warrington, J.A., Anderson, N.N., Park, S.W., Brown, M.S., and Goldstein, J.L. (2003). Combined analysis of oligonucleotide microarray data from transgenic and knockout mice identifies direct SREBP target genes. *Proc. Natl. Acad. Sci. USA* **100**, 12027–12032.
- Huffman, T.A., Mothe-Satney, I., and Lawrence, J.C., Jr. (2002). Insulin-stimulated phosphorylation of lipin mediated by the mammalian target of rapamycin. *Proc. Natl. Acad. Sci. USA* **99**, 1047–1052.
- Jacinto, E., Loewith, R., Schmidt, A., Lin, S., Ruegg, M.A., Hall, A., and Hall, M.N. (2004). Mammalian TOR complex 2 controls the actin cytoskeleton and is rapamycin insensitive. *Nat. Cell Biol.* **6**, 1122–1128.
- Jiang, X., Kenerson, H., Aicher, L., Miyaoka, R., Eary, J., Bissler, J., and Yeung, R.S. (2008). The tuberous sclerosis complex regulates trafficking of glucose transporters and glucose uptake. *Am. J. Pathol.* **172**, 1748–1756.
- Johnson, B.R., Nitta, R.T., Frock, R.L., Mounkes, L., Barbie, D.A., Stewart, C.L., Harlow, E., and Kennedy, B.K. (2004). A-type lamins regulate retinoblastoma protein function by promoting subnuclear localization and preventing proteasomal degradation. *Proc. Natl. Acad. Sci. USA* **101**, 9677–9682.
- Kalaany, N.Y., Gauthier, K.C., Zavacki, A.M., Mammen, P.P., Kitazume, T., Peterson, J.A., Horton, J.D., Garry, D.J., Bianco, A.C., and Mangelsdorf, D.J. (2005). LXRs regulate the balance between fat storage and oxidation. *Cell Metab.* **1**, 231–244.
- Kim, D.H., Sarbassov, D.D., Ali, S.M., King, J.E., Latek, R.R., Erdjument-Bromage, H., Tempst, P., and Sabatini, D.M. (2002). mTOR interacts with raptor to form a nutrient-sensitive complex that signals to the cell growth machinery. *Cell* **110**, 163–175.
- Kim, D.H., Sarbassov, D.D., Ali, S.M., Latek, R.R., Guntur, K.V., Erdjument-Bromage, H., Tempst, P., and Sabatini, D.M. (2003). GbetaL, a positive regulator of the rapamycin-sensitive pathway required for the nutrient-sensitive interaction between raptor and mTOR. *Mol. Cell* **11**, 895–904.
- Lempiäinen, H., Uotila, A., Urban, J., Dohnal, I., Ammerer, G., Loewith, R., and Shore, D. (2009). Sfp1 interaction with TORC1 and Mrs6 reveals feedback regulation on TOR signaling. *Mol. Cell* **33**, 704–716.
- Li, S., Brown, M.S., and Goldstein, J.L. (2010). Bifurcation of insulin signaling pathway in rat liver: mTORC1 required for stimulation of lipogenesis, but not inhibition of gluconeogenesis. *Proc. Natl. Acad. Sci. USA* **107**, 3441–3446.
- Liu, Q., Chang, J.W., Wang, J., Kang, S.A., Thoreen, C.C., Markhard, A., Hur, W., Zhang, J., Sim, T., Sabatini, D.M., and Gray, N.S. (2010). Discovery of 1-(4-(4-propionylpiperazin-1-yl)-3-(trifluoromethyl)phenyl)-9-(quinolin-3-yl)benzo[h][1,6]naphthyridin-2(1H)-one as a highly potent, selective mammalian target of rapamycin (mTOR) inhibitor for the treatment of cancer. *J. Med. Chem.* **53**, 7146–7155.
- Lloyd, D.J., Trembath, R.C., and Shackleton, S. (2002). A novel interaction between lamin A and SREBP1: implications for partial lipodystrophy and other laminopathies. *Hum. Mol. Genet.* **11**, 769–777.
- Moule, S.K., Edgell, N.J., Welsh, G.I., Diggle, T.A., Foulstone, E.J., Heesom, K.J., Proud, C.G., and Denton, R.M. (1995). Multiple signalling pathways involved in the stimulation of fatty acid and glycogen synthesis by insulin in rat epididymal fat cells. *Biochem. J.* **311**, 595–601.
- O'Hara, L., Han, G.S., Peak-Chew, S., Grimsey, N., Carman, G.M., and Siniosoglou, S. (2006). Control of phospholipid synthesis by phosphorylation of the yeast lipin Pah1p/Smp2p Mg²⁺-dependent phosphatidate phosphatase. *J. Biol. Chem.* **281**, 34537–34548.
- Péterfy, M., Phan, J., Xu, P., and Reue, K. (2001). Lipodystrophy in the fld mouse results from mutation of a new gene encoding a nuclear protein, lipin. *Nat. Genet.* **27**, 121–124.
- Péterfy, M., Harris, T.E., Fujita, N., and Reue, K. (2010). Insulin-stimulated interaction with 14-3-3 promotes cytoplasmic localization of lipin-1 in adipocytes. *J. Biol. Chem.* **285**, 3857–3864.
- Peterson, T.R., Laplante, M., Thoreen, C.C., Sancak, Y., Kang, S.A., Kuehl, W.M., Gray, N.S., and Sabatini, D.M. (2009). DEPTOR is an mTOR inhibitor frequently overexpressed in multiple myeloma cells and required for their survival. *Cell* **137**, 873–886.
- Porstmann, T., Santos, C.R., Griffiths, B., Cully, M., Wu, M., Leever, S., Griffiths, J.R., Chung, Y.L., and Schulze, A. (2008). SREBP activity is regulated by mTORC1 and contributes to Akt-dependent cell growth. *Cell Metab.* **8**, 224–236.
- Rehmark, S., Giometti, C.S., Slavin, B.G., Doolittle, M.H., and Reue, K. (1998). The fatty liver dystrophy mutant mouse: microvesicular steatosis associated with altered expression levels of peroxisome proliferator-regulated proteins. *J. Lipid Res.* **39**, 2209–2217.
- Sabatini, D.M., Erdjument-Bromage, H., Lui, M., Tempst, P., and Snyder, S.H. (1994). RAFT1: a mammalian protein that binds to FKBP12 in a rapamycin-dependent fashion and is homologous to yeast TORs. *Cell* **78**, 35–43.
- Sarbassov, D.D., Ali, S.M., Kim, D.H., Guertin, D.A., Latek, R.R., Erdjument-Bromage, H., Tempst, P., and Sabatini, D.M. (2004). Rictor, a novel binding partner of mTOR, defines a rapamycin-insensitive and raptor-independent pathway that regulates the cytoskeleton. *Curr. Biol.* **14**, 1296–1302.
- Schalm, S.S., Fingar, D.C., Sabatini, D.M., and Blenis, J. (2003). TOS motif-mediated raptor binding regulates 4E-BP1 multisite phosphorylation and function. *Curr. Biol.* **13**, 797–806.
- Sengupta, S., Peterson, T.R., Laplante, M., Oh, S., and Sabatini, D.M. (2010). mTORC1 controls fasting-induced ketogenesis and its modulation by ageing. *Nature* **468**, 1100–1104.
- Sharpe, L.J., and Brown, A.J. (2008). Rapamycin down-regulates LDL-receptor expression independently of SREBP-2. *Biochem. Biophys. Res. Commun.* **373**, 670–674.
- Shimano, H., Horton, J.D., Hammer, R.E., Shimomura, I., Brown, M.S., and Goldstein, J.L. (1996). Overproduction of cholesterol and fatty acids causes massive liver enlargement in transgenic mice expressing truncated SREBP-1a. *J. Clin. Invest.* **98**, 1575–1584.
- Shimomura, I., Hammer, R.E., Ikemoto, S., Brown, M.S., and Goldstein, J.L. (1999). Leptin reverses insulin resistance and diabetes mellitus in mice with congenital lipodystrophy. *Nature* **401**, 73–76.
- Singh, K., Sun, S., and Vézina, C. (1979). Rapamycin (AY-22,989), a new antifungal antibiotic. IV. Mechanism of action. *J. Antibiot.* **32**, 630–645.
- Tange, Y., Hirata, A., and Niwa, O. (2002). An evolutionarily conserved fission yeast protein, Ned1, implicated in normal nuclear morphology and chromosome stability, interacts with Dis3, Pim1/RCC1 and an essential nucleoporin. *J. Cell Sci.* **115**, 4375–4385.
- Thoreen, C.C., Kang, S.A., Chang, J.W., Liu, Q., Zhang, J., Gao, Y., Reichling, L.J., Sim, T., Sabatini, D.M., and Gray, N.S. (2009). An ATP-competitive mammalian target of rapamycin inhibitor reveals rapamycin-resistant functions of mTORC1. *J. Biol. Chem.* **284**, 8023–8032.

- Wang, X., Sato, R., Brown, M.S., Hua, X., and Goldstein, J.L. (1994). SREBP-1, a membrane-bound transcription factor released by sterol-regulated proteolysis. *Cell* 77, 53–62.
- Wilson, K.L., and Foisner, R. (2010). Lamin-binding Proteins. *Cold Spring Harb. Perspect. Biol.* 2, a000554.
- Wullschleger, S., Loewith, R., and Hall, M.N. (2006). TOR signaling in growth and metabolism. *Cell* 124, 471–484.
- Yip, C.K., Murata, K., Walz, T., Sabatini, D.M., and Kang, S.A. (2010). Structure of the human mTOR complex I and its implications for rapamycin inhibition. *Mol. Cell* 38, 768–774.
- Yu, L., McPhee, C.K., Zheng, L., Mardones, G.A., Rong, Y., Peng, J., Mi, N., Zhao, Y., Liu, Z., Wan, F., et al. (2010). Termination of autophagy and reformation of lysosomes regulated by mTOR. *Nature* 465, 942–946.